Hindawi
Advances in Materials Science and Engineering
Volume 2019, Article ID 5719694, 9 pages
https://doi.org/10.1155/2019/5719694

Research Article

Impact of High-Velocity Oxy-Fuel ZrO_2 Coating on Corrosion Resistance and Fatigue Life of AISI 316L Austenitic Stainless Steel

J. Jagadesh Kumar[1], **G. Diwakar**[2] **and Vaddi Venkata Satyanarayana**[3]

[1]*Research Scholar, Department of Mechanical Engineering, Koneru Lakshmaiah Education Foundation (Deemed to be University), Vaddeswaram, India*
[2]*Professor, Department of Mechanical Engineering, Koneru Lakshmaiah Education Foundation (Deemed to be University), Vaddeswaram, India*
[3]*Professor, Department of Mechanical Engineering, Vidya Jyothi Institute of Technology, Hyderabad, India*

Correspondence should be addressed to J. Jagadesh Kumar; jagadeshkumar82@gmail.com

Received 27 February 2019; Revised 21 May 2019; Accepted 27 June 2019; Published 30 July 2019

Academic Editor: Guang-xing Liang

Purpose. The purpose of this research paper is to investigate the corrosion and fatigue life of AISI 316L austenitic stainless steel in the absence and presence of high-velocity oxy-fuel ZrO_2 coating. *Design/Methodology/Approach*. AISI 316L austenitic stainless steel is chosen for the investigation, keeping in mind, its widespread usage in naval and marine applications where the members are exposed to corrosive sea water environment. ZrO_2 coating is a popular surface treatment provided to mechanical members to improve their corrosion resistance. Being a refractory material, ZrO_2 inhibits the corrosion of the AISI 316L austenitic stainless steel in marine applications. But, the study of the effect of ZrO_2 coating on the corrosion and fatigue life of the material hitherto is scarce and hence the present investigation is undertaken. The corrosion and fatigue analysis of the coated specimens are carried out by taking two control parameters, namely, rotational speed of job and axial speed of torch, into consideration and applying L4 Taguchi orthogonal array. *Findings*. The corrosion resistance of the material has increased but the fatigue strength has decreased upon coating of ZrO_2 on AISI 316L austenitic stainless steel. The failure has occurred because of the formation of oxide layers on the steel during coating.

1. Introduction

Fatigue failure is the most common failure in mechanical/structural members and the fatigue life of any component is influenced by its internal design aspects and external factors like the environment, operating temperature, etc. Corrosion fatigue analysis is the study of the combined effect of corrosion and fatigue on the life of a component, and it emerged as a separate branch in fatigue analysis due to the profound impact of the corrosion on fatigue life of a member. Since it is a combined effect of fatigue and corrosion, corrosion fatigue can bring in a far greater deprivation in strength than either effect acting alone or by superposition of the singular effects. Shin et. al. proved that ZrO_2-SiO_2 coatings increase the resistance of AISI 316L stainless steel against corrosion [1]. Bačić et. al. demonstrated that, by providing sol-gel Yttria Stabilized ZrO_2 films sintered at 400°C to AISI 316L austenitic stainless steel, the corrosion resistance significantly improved in 3.5 wt.% NaCl aqueous solution [2]. Kazazi et al. investigated the impact of ZrO_2 sol-sel Coating on 316L stainless steel in nitric acid solution and concluded that the corrosion resistance has improved considerably by providing ZrO_2 coating [3].

Nascimento et al., in their research mentioned that the effect of tungsten carbide thermal spray coating applied by HP/HVOF process and hard chromium electroplating decreased the fatigue strength of AISI 4340 steel [4]. Surface treatment is one of the most promising methods, to improve corrosion fatigue strength of structural materials, in service environments [5]. Ebara concluded that corrosion fatigue

life of KA32 (thermo-mechanically controlled processed) steel and welded joints can be improved greatly, by coating with tar epoxy resins [6]. Puntambekar et al. proposed that thermal spray treatment of alumina and zirconia results in decrement in fatigue life of EN-24 steel [7].

The primary emphasis of the present work is to investigate the corrosion resistance and fatigue life of AISI 316L austenitic stainless steel with and without coating of ZrO_2 on it. AISI 316L austenitic stainless steel is chosen for the investigation, keeping in mind, its widespread usage in naval and marine applications where the members are exposed to corrosive sea water environment. ZrO_2 coating is a popular surface treatment provided to mechanical members to improve their corrosion resistance. Being a refractory material, ZrO_2 inhibits the corrosion of the AISI 316L austenitic stainless steel in marine applications. But, the study of the effect of ZrO_2 coating on the corrosion resistance and fatigue life of the material hitherto is scarce, and hence, the present investigation is undertaken. The corrosion and fatigue analysis of the coated specimens is carried out by taking two control parameters namely rotational speed of job and axial speed of torch into consideration and applying L4 Taguchi orthogonal array. The results are further subjected to analysis of variance (ANOVA) as per Yate's algorithm to arrive at the contribution of each parameter.

2. Materials & Methods

2.1. Material. AISI 316L austenitic stainless steel is the material for which the corrosion resistance and fatigue life are analyzed in the current research. This steel is primarily used in naval and marine applications as it possesses excellent corrosion resistance and high strength to weight ratio. The chemical composition and mechanical properties of the material used are given in Tables 1 and 2, respectively.

2.2. HVOF Coating. The chosen material is coated with ZrO_2 by employing a high-velocity oxy-fuel torch machine (Figure 1). ZrO_2 is passed through the central orifice of the torch and fuel gas mixed with oxygen passes through the conduit of the torch. After getting heated at the tip of the torch, the molten ZrO_2 is sprayed on to the job so that it gets coated on the specimen.

2.3. Design of Experiments. The machine employed for coating has the capacity of changing speed of coating on the specimen by varying the rotational speed of the specimen and linear axial speed of the HVOF torch. Table 3 depicts the factors chosen at two levels each in the current investigation. Further, L4 Taguchi orthogonal array [8] as shown in Table 4 is chosen for experimentation.

2.4. Fatigue Testing Machine. A Plug-N-Play Fatigue Testing Machine from ITW (Figure 2) is employed for finding the fatigue life of the specimens. The machine has the provision to apply alternate tensile and compressive axial reversed loads. It is provided with a computer data logger to record the number of cycles applied during the test.

2.5. Fatigue Specimen. The scope of the current research includes the comparison of fatigue life of uncoated and ZrO_2-coated specimens before and after corrosion, subjected to axial loading by the Fatigue Testing Machine. The specimens employed for the investigation are depicted in Figure 3. The specimens are fabricated as per ASTM E606 standards using a CNC lathe.

2.6. Corrosion Testing. The uncoated and ZrO_2-coated specimens are tested for pitting corrosion in an electrolyte of 0.5 M H_2SO_4 + 0.5 M HCl. The electrochemical measurements were made using a potentiometer after 10 minutes of dipping in the electrolyte. The potential at which the current increases abruptly after the passive region was taken as the pitting potential. Specimens that exhibit higher positive potential value are considered to be having better pitting resistance.

2.7. Scanning Electron Microscopy (SEM). Scanning electron microscope was used to examine the fractured features from failed fatigue specimens at various magnifications. The samples of required sizes were cut and prepared. The samples prepared were ultrasonically cleaned and degassed before putting in SEM chamber.

2.8. X-Ray Diffraction. The XRD patterns are observed by employing X-ray diffractometer with CuKα radiation, and thereby, the morphology of the ZrO_2 coated surface of the specimen is analyzed.

2.9. Methodology of Experimentation. The specimens so chosen are coated with ZrO_2 and subjected to corrosion and fatigue tests. They are compared and evaluated with uncoated counterparts. The methodology undertaken in the research is shown in Figure 4.

3. Results & Analysis

The AISI 316L Austenitic stainless steel specimens were tested for low-cycle fatigue at a constant strain rate of $3 \times 10^{-3}\,s^{-1}$. The experiments were performed for two specimens in each case for the sake of consistency and error reduction. Table 5 shows the fatigue life of the uncoated specimen.

The specimens of AISI 316L austenitic stainless steel were coated with ZrO_2 using two control parameters (Table 3) as per the Taguchi experimental array. The thickness of the coating is in the range of 300 μm to 400 μm for the experimental runs specified in Table 6. The SEM micrograph and XRD pattern of the ZrO_2 coated surface are given in Figure 5. These specimens are taken up for fatigue life estimation at a stress of 250 MPa and a strain rate of $3 \times 10^{-3}\,s^{-1}$ (Table 6).

Table 1: Chemical composition (wt.%).

Element	C	Mn	Si	Cr	Ni	Mo	P	S	N	Fe
%	0.03	2	0.75	17.00	12.00	2.5	0.045	0.03	0.1	Balance

Table 2: Mechanical properties.

Hardness (BH)	UTS (MPa)	Yield strength (MPa)	Elongation (%)	Elastic modulus (GPa)
146	560	235	55	193

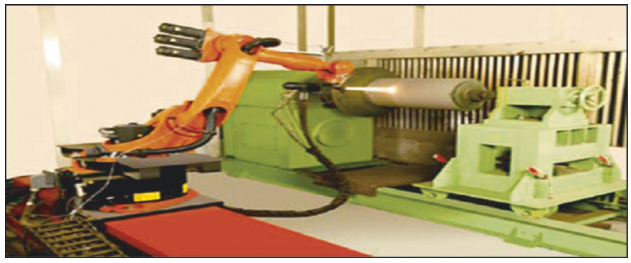

Figure 1: Round bars being HVOF sprayed while mounted onto the mandrel.

Table 3: Factors chosen at their levels.

Factor	Notation	Units	Levels	
			Low (1)	High (2)
Rotational speed of job	x_1	rpm	50	70
Axial speed of torch	x_2	mm/min	300	500

Table 4: L4 Taguchi orthogonal array.

Run	x_1	x_2
1	1	1
2	1	2
3	2	1
4	2	2

The data have been subjected to standard analysis of variance (ANOVA) as per Yate's algorithm [9, 10]. The analysis of variance is computed with a scale of 10,000 cycles for the data of the coated specimens, and the contribution of each factor has been evaluated (Table 7).

In order to find their corrosion resistance, the specimens were tested for their pitting potential employing a potentiometer. Tables 8 and 9 give the pitting potential (mV) of the specimens tested.

Similarly, the specimens which were subjected to corrosion were taken for fatigue testing under the same test conditions. Tables 10 and 11 illustrate the fatigue life of the corroded specimens of uncoated and coated jobs, respectively. The ZrO_2-coated 316L austenitic stainless steel-corroded specimen after failure is shown in the Figure 6.

Figure 2: Specimen mounted on the Plug-N-Play Fatigue Testing Machine.

4. Discussion

Lowest value of coating thickness is observed for the Run 4 due to higher traversal speed of the torch and higher rotational speed of the job. The XRD pattern indicates a monoclinic crystalline structure of ZrO_2. The coating is done at high temperatures in the range 1300°C–1500°C, and the crystalline structure changed from monoclinic to tetragonal during the coating process; however, during cooling, the crystalline structure returned back to be monoclinic (Figure 5(b)). Due to the difference in the coefficient of thermal expansion between the parent material and coating, there is a change in volume which causes microporosity as exhibited in the SEM micrograph (Figure 5(a)). It is observed that coating of ZrO_2 on the AISI 316L austenitic stainless steel has reduced the fatigue life. The formation of high-density oxide inclusions which occurred during the coating process have become the sites for formation of cracks and subsequent speedy propagation of these cracks while testing for the fatigue life and hence resulted in lower

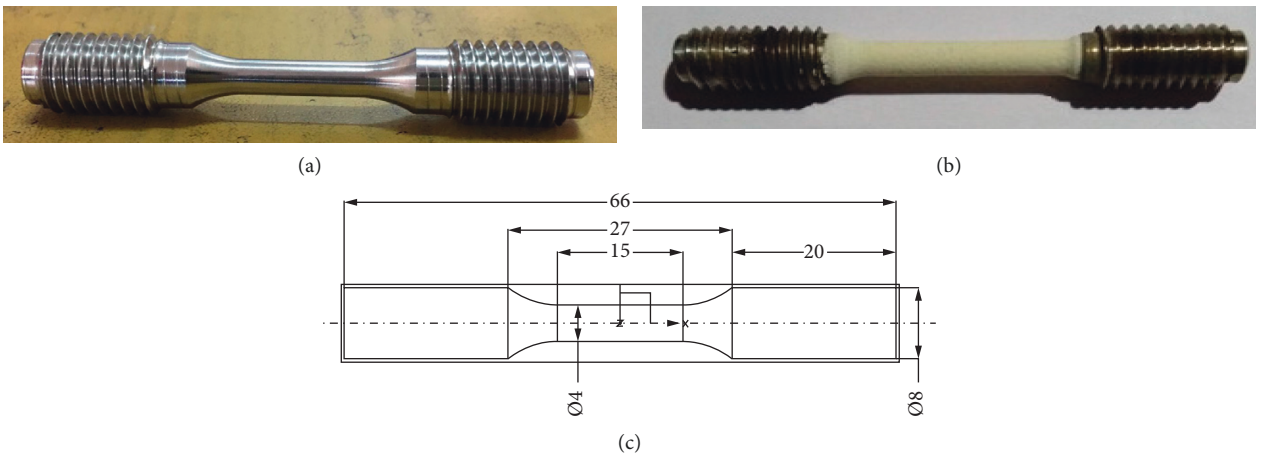

Figure 3: Fatigue specimens. (a) AISI 316L standard fatigue specimen. (b) AISI 316L fatigue specimen with 300 μm ZrO_2 coating. (c) Standard fatigue specimen drawing.

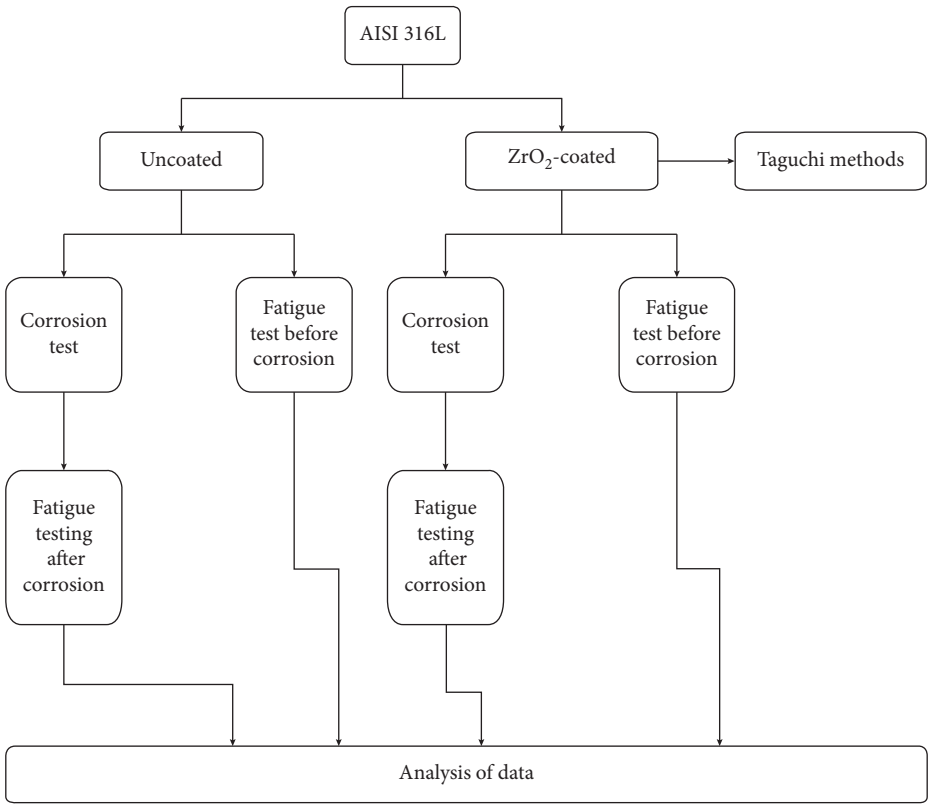

Figure 4: Methodology of experimentation.

Table 5: Fatigue life (cycles) of uncoated AISI 316L austenitic stainless steel specimen.

S. no.	Test condition			Fatigue life (cycles)	
	Stress (MPa)	Strain amplitude (%)	Strain rate	Trial 1	Trial 2
1	250	0.4	$3\times10^{-3}\,s^{-1}$	11227	11212

Table 6: Fatigue life (cycles) of ZrO_2-coated AISI 316L austenitic stainless steel specimen.

Run	Factor x_1	Factor x_2	Test conditions	Fatigue life (cycles)	
				Trail 1	Trial 2
1	1	1	Stress 250 MPa Strain amplitude 0.4% Strain rate $3\times10^{-3}\,s^{-1}$	10692	10685
2	1	2		10740	10745
3	2	1		10710	10712
4	2	2		11000	11020

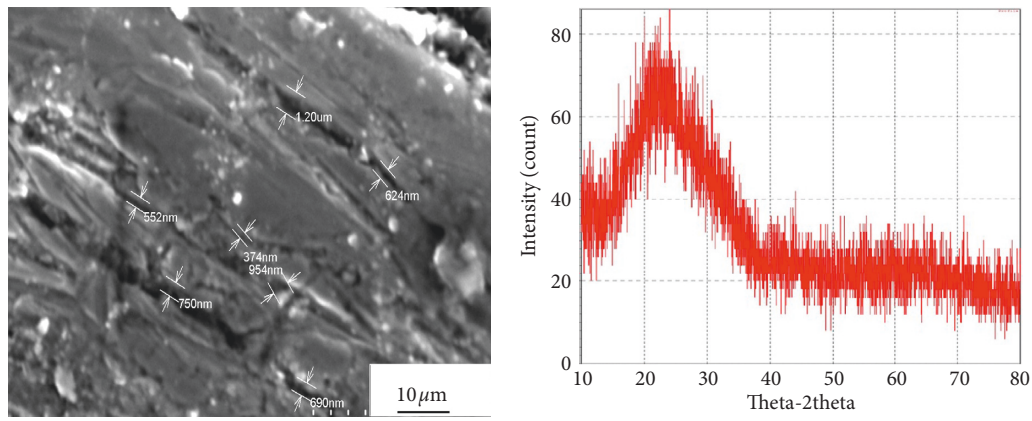

(a) (b)

Figure 5: Morphology of coated surface. (a) SEM micrograph. (b) XRD pattern.

Table 7: ANOVA computations for fatigue life of ZrO_2-coated specimens.

Source	Sum of squares	DOF	Mean square	Fisher ratio	% contribution
x_1	0.0004234	1	0.0004234	4.775	8.84
x_2	0.00062658	1	0.00062658	7.067	14.18
x_3 $(x_1 * x_2)$	0.0023814	1	0.0023814	26.85	60.55
Error	0.00035462	4	0.00008866	—	—
Total	0.003786	7	—	—	—

Table 8: Corrosion test results of uncoated specimens.

Pitting potential (mV)	
Trial 1	Trial 2
911	916

Table 9: Corrosion test results of coated specimens.

Run	x_1	x_2	Pitting potential (mV)	
			Trial 1	Trial 2
1	1	1	1015	1020
2	1	2	1011	1015
3	2	1	1010	1015
4	2	2	1010	1008

Table 10: Fatigue life (cycles) of uncoated AISI 316L austenitic stainless steel corroded specimen.

S. no	Test conditions			Fatigue life	
	Stress	Strain amplitude (%)	Strain rate	Trail 1	Trial 2
1	250	0.4	$3\times10^{-3}\,s^{-1}$	11106	11102

life compared to the uncoated specimen (Figure 7). At a slow speed of rotation of gun, the specimen is exposed to high heat inputs and more amounts of ZrO_2 coatings, and hence, it exhibited lower fatigue life and higher pitting potential. From the ANOVA computations as shown in Table 7, it can be concluded that the interaction effect of both the governing factors have profound effect (60.55%) on the coating and subsequently the fatigue life of the specimen.

Table 11: Fatigue life (cycles) of ZrO_2-coated 316L austenitic stainless steel corroded specimen.

Run	Factor x_1	Factor x_2	Test conditions	Fatigue life (cycles)	
				Trial 1	Trial 2
1	1	1	Stress 250 (MPa) Strain amplitude 0.4% Strain rate $3\times10^{-3}\,s^{-1}$	9895	9900
2	1	2		9930	9940
3	2	1		9935	9945
4	2	2		9948	9950

Figure 6: ZrO_2-coated 316L austenitic stainless steel-corroded specimen after failure.

The fatigue life of the specimens that are not subjected to corrosion, on which coating is performed at high axial speed of the torch and high rotational speed of the job, is found to be higher than that of the specimen coated with the same parameters at their minimum levels. It is owing to the reason of having lower thickness of coat formed on the specimen at higher axial speed of the torch and rotational speed of the job. Similarly, the test run with rotational speed at lower level and axial speed of the torch at higher level has resulted in a midlevel fatigue life between the above two extreme cases.

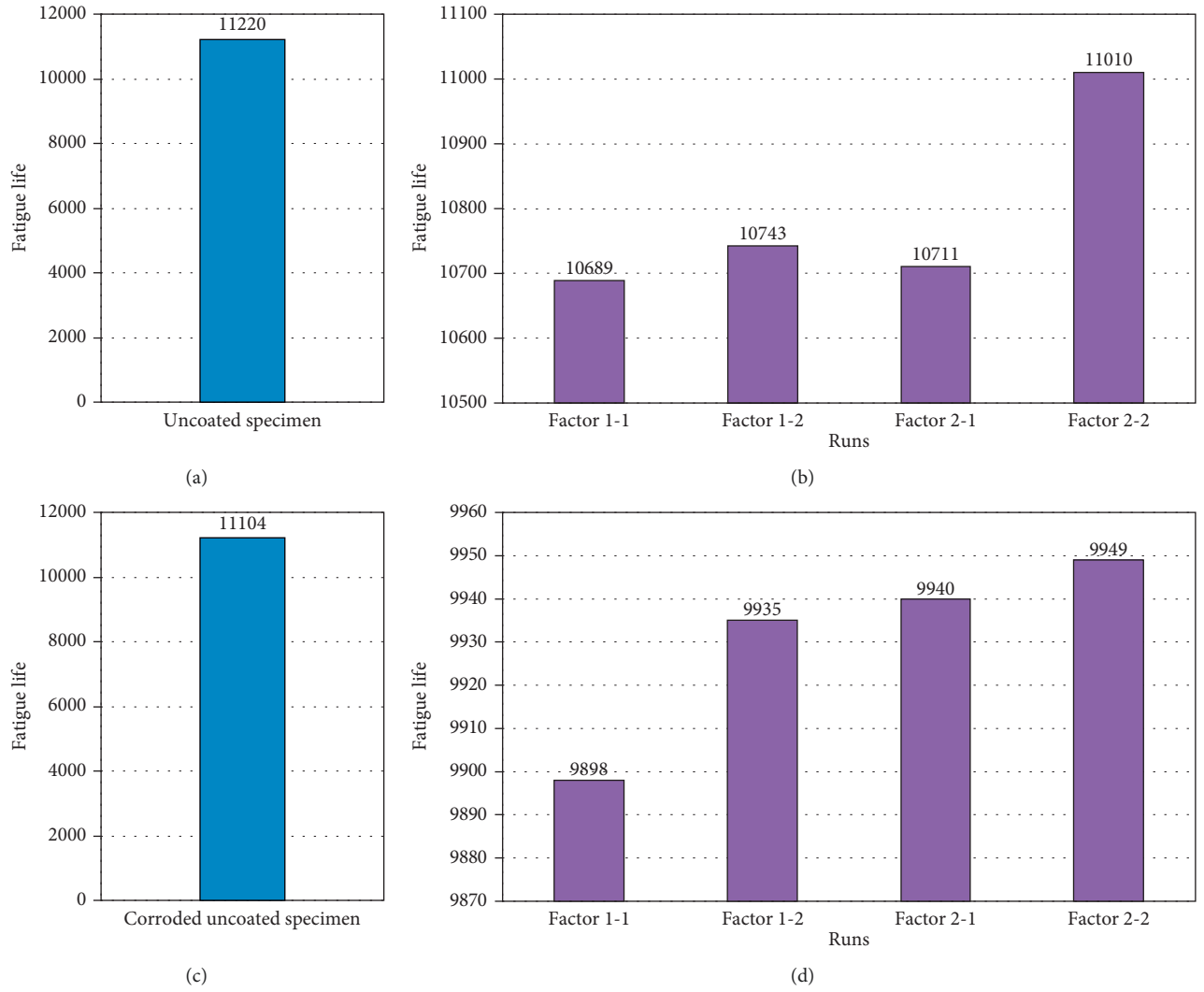

Figure 7: Average fatigue life (cycles) of AISI 316L stainless steel. (a) Uncoated specimen and (b) coated specimen before corrosion. (c) Uncoated specimen and (d) coated specimen after corrosion.

Hence, the optimal condition can be taken as the one which has both the parameters at their higher levels. The fatigue run results show that the axial speed of the torch has higher influence on the thickness of the coating and consequently on the fatigue life of the specimen which is corroborated further with a contribution of 14.18% as shown in Table 7.

It is clearly evident from the results that, for both the coated and uncoated specimens, the fatigue life had reduced due to corrosion. For the uncoated specimens, the fatigue life declined from 11220 to 11104 cycles which is about 1.03% drop while at the optimal parameter condition of coating, the fatigue life decreased from 11010 to 9949 cycles to an abnormal extent of 9.64%, due to corrosion.

The plots for pitting potential of AISI 316L austenitic stainless steel for uncoated and coated specimens are shown in Figure 8. The oxide layer formed on the surface of the specimen is prone to corrosion, and hence, pitting potential of the coated specimens was reduced despite the parent material possessing higher corrosion resistance.

The uncoated specimen had a pitting potential of 914 mV while, for the specimen coated at the optimum coating condition for fatigue life (higher axial speed of the torch and higher rotational speed of the job) the pitting potential increased to 1009 mV. However, it is evident from the Figure 7 that the optimum coating condition for pitting potential is, lower axial speed of the torch and lower rotational speed of the job. This is due to the fact that, at lower speeds, the coating thickness would increase on the specimens which in turn enhance the corrosion resistance. The optimal parameter condition for the fatigue life and corrosion resistance is different when they are observed in isolation. To have a combined optimal parameter condition which maximizes both responses simultaneously, a modified Taguchi analysis is carried out [11, 12]. Signal-To-Noise ratios (S/N) are computed with "higher the better" quality characteristics giving equal weightage to the responses as given in Table 12 and are subjected to analysis of means which are plotted in Figure 9.

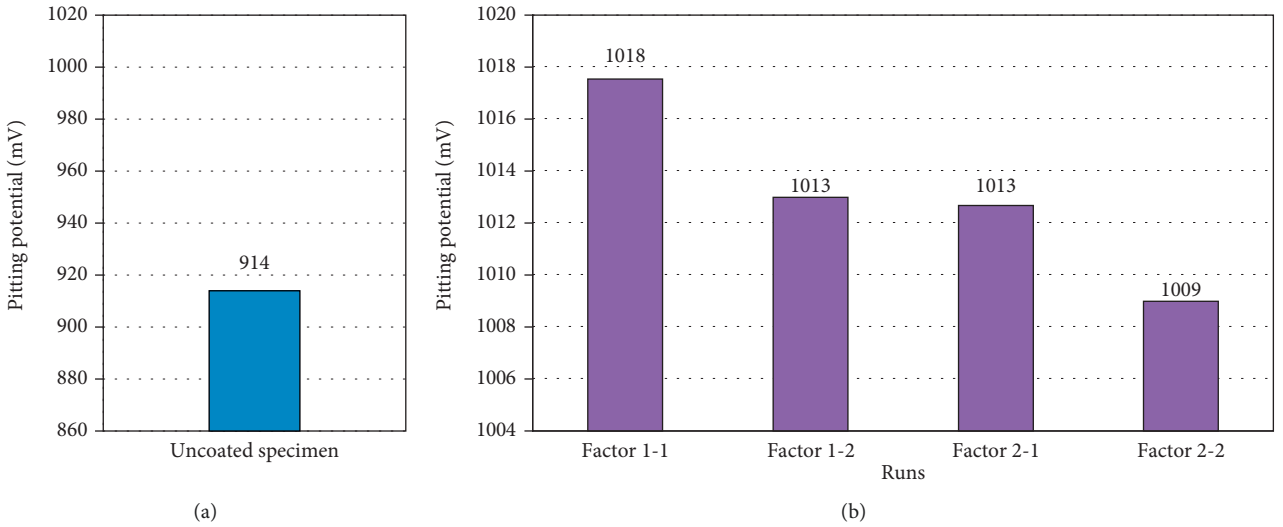

Figure 8: Average pitting potential of AISI 316L stainless steel. (a) Uncoated specimen. (b) Coated specimen.

Table 12: S/N ratio for the combined responses.

Run	Factor x_1	Factor x_2	Average pitting potential (mV)	Average fatigue life (cycles)	Weighted average	S/N ratio (dB)
1	1	1	1017.5	9897.5	5966.25	75.51
2	1	2	1013	9935	5980.5	75.53
3	2	1	1012.5	9940	5982.5	75.54
4	2	2	1009	9949	5983.5	75.54

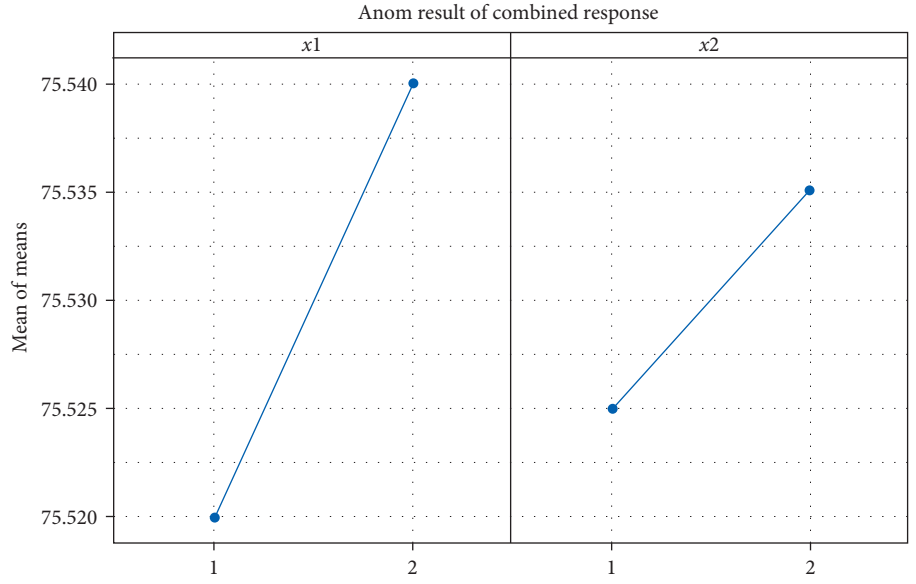

Figure 9: S/N plot for the combined responses.

The combined optimal parameter condition is computed, for both the responses by giving equal weightage to the fatigue life and corrosion resistance, by taking higher S/N ratio. It is found that when rotational speed and axial speed of the torch are at higher levels, the optimal condition is reached.

When it comes to real-time applications of austenitic stainless steels, for components of marine and naval structures, improvement in corrosion resistance is of more significance when compared to the marginal decline in the fatigue life due to surface coating with ZrO_2. This is due to the inherent corrosive environment in which the structure operates.

Scanning electron micrographs of uncoated and coated specimens are shown in Figure 10. The fractured surface of the coated uncorroded specimen in

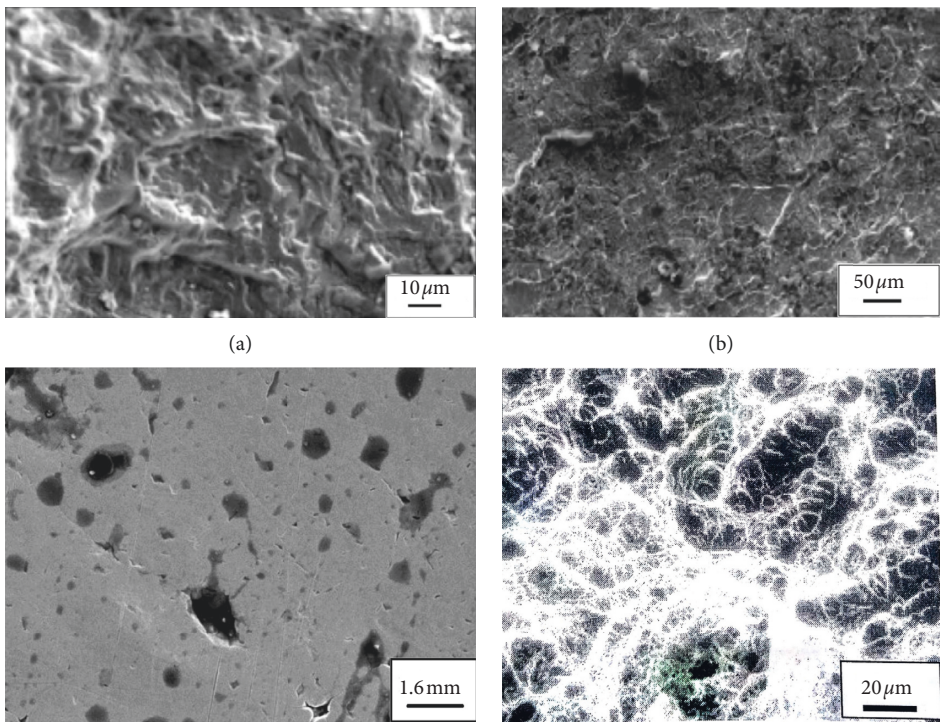

Figure 10: Scanning electron micrographs. Fractured surface of (a) uncoated uncorroded specimen, (b) uncoated corroded specimen, (c) coated uncorroded specimen, and (d) coated corroded specimen.

Figure 10(c) shows the porosity sites of oxides corroborating the early formation of crack and fast propagation resulting in reduced fatigue life. The micrograph portrays the fracture to be brittle coupled with the oxide layer spots. The fracture surface is flat and has large facet size which implies lower ductility. This may be attributed to the oxide layer spots formed during coating process. It can also be observed from Figures 10(b) and 10(d) that a brittle type of fracture occurred in both scenarios of corroded specimens.

5. Conclusions

(i) Coating of ZrO_2 on the AISI 316L austenitic stainless steel has reduced the fatigue life. However, corrosion resistance of the material has considerably increased due to coating.

(ii) High-velocity oxy-fuel coating method employed, resulted in formation of oxide layers on the substrate material and consequently has reduced fatigue life of the parent metal.

(iii) For the uncoated specimens, the fatigue life declined from 11220 to 11104 cycles, which is about 1.03% drop while at the optimal parameter condition of coating; the fatigue life decreased from 11010 to 9949 cycles which is in the tune of 9.64%, due to corrosion.

(iv) From the modified Taguchi analysis, it is found that the control parameters at their higher levels yielded the combined optimal parameter condition.

Abbrevations

ZrO_2: Zirconia/zirconium dioxide
HVOF: High-velocity oxy-fuel
LCF: Low-cycle fatigue
ANOVA: Analysis of variance
EM: Elastic modulus
UTS: Ultimate tensile strength
YS: Yield strength
BH: Brinell hardness
SEM: Scanning electron microscope
XRD: X-ray diffractometer.

Data Availability

The data used to support the findings of this study are available from the corresponding author upon request.

Conflicts of Interest

The authors declare that there are no conflicts of interest pertinent to the current research paper.

Acknowledgments

The authors would like to thank Dr. G. Sreeram Reddy and Dr. B.V. Reddi, Department of Mechanical Engineering, V.J.I.T., Hyderabad, for giving valuable suggestions during the execution of work. The authors also express their deep sense of gratitude towards Dr. P. Ravinder Reddy, Principal, C.B.I.T., Hyderabad, for providing permission to conduct experiments at C.B.I.T.

References

[1] D. Y. Shin, K. N. Kim, I.-T. Nam, and S. M. Han, "Improvement of corrosion resistance of stainless steel by ZrO_2-SiO_2 sol-gel coatings," *Materials Science Forum*, vol. 510-511, pp. 442–445, 2006.

[2] I. Bačić, H. O. Ćurković, L. Ćurković, V. Mandić, and Z. Šokčević, "Corrosion protection of AISI 316L stainless steel with the sol-gel yttria stabilized ZrO_2 films: effects of sintering temperature and doping," *International Journal of Electrochemical Science*, vol. 11, pp. 9192–9205, 2016.

[3] M. Kazazi, M. Haghighi, D. Yarali, and M. H. Zaynolabedini, "Improving corrosion resistance of 316L austenitic stainless steel using ZrO_2 sol-gel coating in nitric acid solution," *Journal of Materials Engineering and Performance*, vol. 27, no. 3, pp. 1093–1102, 2018.

[4] M. P. Nascimento, R. C. Souza, I. M. Miguel, W. L. Pigatin, and H. J. C. Voorwald, "Effects of tungsten carbide thermal spray coating by HP/HVOF and hard chromium electroplating on AISI 4340 high strength steel," *Surface and Coatings Technology*, vol. 138, no. 2-3, pp. 113–124, 2001.

[5] J. Jagadesh Kumar, G. Diwakar, and V. V. Satyanarayana, "Corrosion fatigue of welded joints in marine and naval structures: a review," *International Journal of Mechanical and Production Engineering Research and Development*, vol. 7, no. 6, pp. 155–162, 2017.

[6] R. Ebara, "Corrosion fatigue behavior of ship hull structural steels," in *Proceedings of the International Coach Federation (ICF10)*, vol. 32, Honolulu, Hawaii, USA, October 2001.

[7] U. N. Puntambekar, G. S. Grewal, P. B. Joshi, and P. Sampathkumaran, "Effect of thermal spray on fatigue life of low-alloy steel," *International Journal of Latest Research in Science and Technology*, vol. 3, no. 4, pp. 132–137, 2014.

[8] G. Taguchi, *System of Experimental Design*, John Wiley & Sons, New York, NY, USA, 1987.

[9] K. Hinkelmann and O. Kempthorne, *Design and Analysis of Experiments*, John Wiley & Sons, NewYork, NY, USA, 1966.

[10] V. V. Satyanarayana, G. Madhusudhan Reddy, and T. Mohandas, "Continuous drive friction welding studies on AISI 304 austenitic stainless steel welds," *Materials and Manufacturing Processes*, vol. 19, no. 3, pp. 487–505, 2004.

[11] V. V. Satyanarayana, G. Madhusudhan Reddy, and K. Veladri, "Application of modified Taguchi method in process parameter selection of the shell moulding process," *Indian Foundry Journal*, vol. 53, no. 10, pp. 37–40, 2007.

[12] G. Sreeram Reddy, M. Hussian, and V. V. Satyanarayana, "Experimental investigation to optimize parameters of reverse engineering technology for reconstructing freeform surfaces," *International Journal of Mechanical Engineering and Technology*, vol. 7, no. 4, pp. 165–174, 2016.